

University of Texas Rio Grande Valley

ScholarWorks @ UTRGV

Manufacturing & Industrial Engineering Faculty
Publications and Presentations

College of Engineering and Computer Science

7-2022

A Numerical Study on the Powder Flowability, Spreadability, Packing Fraction in Powder Bed Additive Manufacturing

Yeasir Mohammad Akib

Ehsan Marzbanrad

Farid Ahmed

Jianzhi Li

Follow this and additional works at: https://scholarworks.utrgv.edu/mie_fac



Part of the [Industrial Engineering Commons](#), and the [Manufacturing Commons](#)

MSEC2022-85323

A NUMERICAL STUDY ON THE POWDER FLOWABILITY, SPREADABILITY, PACKING FRACTION IN POWDER BED ADDITIVE MANUFACTURING

Yeasir Mohammad Akib

Dept. of Manufacturing and Industrial Engineering, The University of Texas Rio Grande Valley, Edinburg, TX 78539

Ehsan Marzbanrad

Dept. of Mechanical and Mechatronics Engineering, University of Waterloo, Waterloo, Ontario, Canada, N2L 3W8

Farid Ahmed*

Dept. of Manufacturing and Industrial Engineering, The University of Texas Rio Grande Valley, Edinburg, TX 78539
farid.ahmed@utrgv.edu

Jianzhi Li

Dept. of Manufacturing and Industrial Engineering, The University of Texas Rio Grande Valley, Edinburg, TX 78539

ABSTRACT

The powder bed fusion (PBF) process is widely adopted in many manufacturing industries because of its capability to 3D print complex parts with micro-scale precision. In PBF process, a thermal energy source is used to selectively fuse powder particles layer by layer to build a part. The build quality in the PBF process primarily depends on the thermal energy deposition and properties of the powder bed. Powder flowability, powder spreading, and packing fraction are key factors that determine the properties of a powder bed. Therefore, the study of these process parameters is essential to better understand the PBF process. In our study, we developed a two-dimensional powder bed model using the granular package of the LAMMPS molecular dynamics simulator. Cloud-based deposition was adopted for pouring powder particles on the powder bed. The spreading of particles over the substrate was mimicked like a powder bed system. The powder flowability in the proposed study was analyzed by varying the particle size distribution. The simulation results showed that a greater number of larger particles in a power sample results in an increase in the Angle of Repose (AOR) which ultimately affects the flowability. Two different kinds of recoater geometry were considered in this study: circular and rectangular blades. Simulation results showed that depending on the recoater shape there is a change in the packing fraction in the powder bed. Cross-sectional analysis of the powder bed

showed a significant presence of voids when a greater number of larger particles existed in the powder batch. The packing fraction of the powder bed was found to be a strong function of particle size distribution. These analyses help understand the influence of particle size and recoater shape on the powder bed properties. Findings from this study help to provide a guideline for choosing particle size distribution if the spherical particles are considered. While the present study focuses on the spherical powder particles, the proposed system can also be adapted to the study of powder bed with aspherical particles.

Keywords: Powder Bed Fusion (PBF), Powder Flowability, Spreadability, Packing Fraction, Molecular Dynamics (MD) Simulation

NOMENCLATURE

PBF	Powder Bed Fusion
MD	Molecular Dynamics
LAMMPS	Large-scale Atomic Molecular Massively Parallel Simulator
DEM	Discrete Element Method
AOR	Angle of Repose
OVITO	Open Visualization Tool

1. INTRODUCTION

Many industries are currently revolutionized by the Additive Manufacturing process because of its capability to produce operatable parts. Powder bed fusion process, an additive manufacturing technique that has drawn much attention to researchers nowadays. As a heat source in the powder bed fusion process, a laser or electron beam is used in general. All types of PBF include spreading powder over the bed periodically to build a new layer. Powders can be provided on the bed by either a hopper or a feed cartridge of a certain height. Fabrication of parts is dependent on many process parameters like laser-related, scan-related, powder-related, and temperature-related [1]. Improvement of powder bed density and homogeneity can decrease the melting defects of the powder bed and improve the part quality [2][3][4]. Denser powder layers make some powder fusion processes (Electron beam selective melting [5][6] and Selective laser melting [7][8]) more steady and continuous. Other defects such as porosity, balling effect, geometric defects, surface defects, microstructural inhomogeneity also contributed to the overall quality of the bed [9]. Indeed these defects are dependent on different sources like equipment, process, design for additive choices, and feedstock materials [9].

In the PBF process, one of the most important concerns is to choose a suitable particle size and size distribution [10]. Choice of particle size is also important as it affects the layer thickness. When particle sizes are greater, it is usually possible to achieve a higher density as the smaller particles can fit in between the larger particles, creating a higher density bed [11]. In the PBF, smaller particles are desired as it attributes to better dimensional accuracy. Small particle size reduces surface roughness [12][11], and particle packing [13][14]. However, porosity increases when the particle sizes are drawn to a very small scale (micron) [15]. So, it's crucial to choose a good particle size with the size distribution.

Granular particles are composed of many dissipative particle-body interactions which can be handled by using MD simulation. MD simulation aids to understand the motion of particles in a system. Since experimental measurement of the flow of powder particles in the powder bed is arduous work, we can get a good understanding of flow using the MD simulation. Some studies have been done regarding the powder particle properties, their spreading process during the additive manufacturing process [16]. Most of those works include the Discrete Element Method (DEM), which is a well-established modeling technique for large-scale small particles. Parteli and Pöschelb [17] found out that process speed can impact the roughness of powder beds. Chen et al. [18] show that DEM simulation can give a clear understanding of the relationship between the layering parameters with the powder bed. DEM algorithms are very similar to MD simulation [19] in many ways with the advantage of using parallel computing for

simulating a large system of particles. Many researchers used both of the terms interchangeably [20]. In this paper, we used MD simulation to investigate the powder bed system. To the authors' best knowledge there is no article yet where the distribution of polydisperse particles in the final bed with multilayer pouring is presented. The basic granular pouring method from the LAMMPS website is used for developing the simulation model. We observed the influence of some process parameters on the final bed. The simulation was carried out in the lab computer which has an Intel® Core™ i5 – 8th generation processor with 16 GB RAM.

2. METHODOLOGY AND SIMULATION SETUP

The model was built up using the Large-scale Atomic/Molecular Massively Parallel Simulator (LAMMPS) [21] and visualization was done by Open Visualization Tool (OVITO) [22]. A serial version (29 Sep 2021) of LAMMPS was used to perform the simulation. As an initialization, we set the boundary to two dimensions. Periodic boundary condition was applied to the z-axis whereas the x-axis was non-periodic (fixed) and the y-axis was non-periodic (shrink-wrapped). The particles were treated as a finite-sized spheres with different diameters. Microcanonical ensemble NVE was used to update the position, angular velocity, and velocity of the spherical particles. As a pair style, we have used gran/hertz/history to calculate the frictional force between two granular particles [23][24][25]. This pair style works when the distance r is less than the contact distance $d = R_i + R_j$ between two different particles (R_i, R_j is the radius of two different particles). The Hertzian style equation (Eqn. 1) is shown below:

$$\begin{aligned}
 F_{hz} &= \sqrt{\delta} * \sqrt{\frac{R_i R_j}{R_i + R_j}} * F_{hk} \\
 &= \sqrt{\delta} * \sqrt{\frac{R_i R_j}{R_i + R_j}} * [(k_n \delta n_{ij} - m_{eff} \gamma_n v_n) - (k_t \Delta s_t + m_{eff} \gamma_t v_t)]
 \end{aligned} \tag{1}$$

Parameters used in equation (1) are:

k_n = Elastic constant for normal contact

k_t = Elastic constant for tangential contact

δ = Overlap distance of two particles

γ_n = Viscoelastic damping constant for normal contact

γ_t = Viscoelastic damping constant for tangential contact

Δs_t = Tangential displacement vector between two particles (Truncated)

m_{eff} = Effective mass of two particles with M_i and M_j mass

n_{ij} = Unit vector that connects centerline of two particles

v_n = Normal component of the relative velocity of two particles

v_t = Tangential component of the relative velocity of two particles

Parameter values used in our model are shown in table 1:

Table 1: Pair style parameter value for the simulation

k_n	k_t	γ_n	γ_t	xmu	$damflag$
4000	NULL*	350	NULL*	0.5	0*

$$* k_t = \text{NULL} = \left(\frac{2}{7}\right) * k_n$$

$$\gamma_t = \text{NULL} = \left(\frac{1}{2}\right) * \gamma_n$$

$damflag = 0$, which means tangential damping force is excluded.

$xmu = F_t/F_n$ = Static yield criterion

$$k_n = \frac{4 * G}{3(1 - nu)}$$

$$k_t = \frac{4 * G}{(2 - nu)}$$

$$G = \frac{E}{2(1 + nu)}$$

E = Young's Modulus

G = Shear Modulus

nu = Poisson's ratio

Values in table 1 were set properly to mimic the ideal powder flow in the powder bed system. The gravity was set to three times the general gravity to adjust the jumping effect of the particles. At the base gravity, the powder particles were pouring like Ping-Pong balls.

The geometric region was set to -0.5 to 0.5 in the z -axis. This is customary to keep z -axis finite for a 2D simulation in LAMMPS. We used the square lattice style with 0.95 lattice constant in our simulation. After constructing the regions, an array of atoms was used to build the powder bed and the recoater (Both circular and blade shape) by using the Create_atoms command in LAMMPS. Velocities of the atoms in the z -direction were zeroed by using the fix enforce2d command. We applied the frictional wall at both sides of the x and y -direction to simulate the granular system. Pairwise force field coefficients were set to asterisks. Timestep used for our study was 0.001. A total of 10 times particle spreading over the powder bed was adopted in our simulation. A snapshot of our powder bed is shown below.

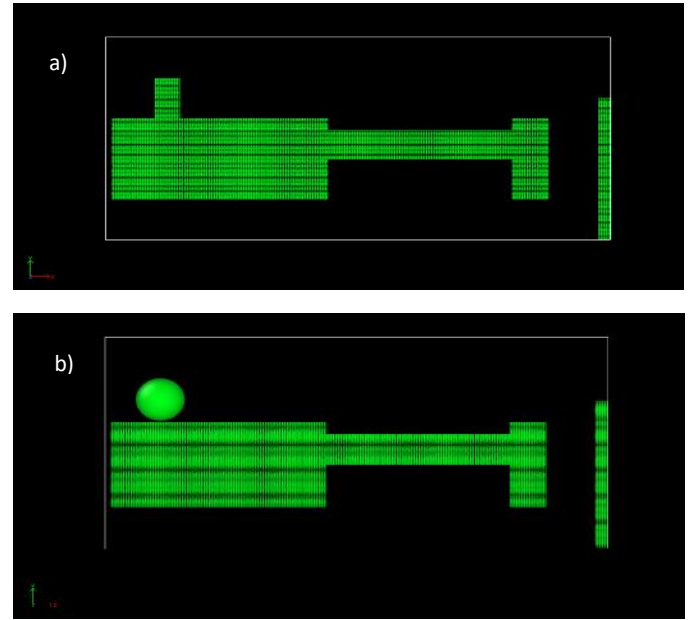


FIGURE 1: a) Powder bed with blade recoater b) Powder bed with circular recoater

3. RESULTS AND DISCUSSION

In this section, we observed the influence of some process parameters on the powder bed system.

3.1 Angle of Repose (AOR)

Angle of Repose characterizes the interparticle friction during the movement of bulk powder materials. A higher angle of repose means poor flowability and vice-versa. In this paper, we investigate the effects of different sized particle ratios on AOR. A total of seven types of different diameter particles were used for our calculation. Powders were poured from a narrow opening of the upper portion of the bed which mimics a funnel method [26]. ISO-4490 defined angle of repose as the free flow of powder particles through a funnel [27]. Angle of Repose (AOR) was calculated by using the following formula (Eqn. 2):

$$\theta = \tan^{-1} \frac{2 * h}{d} \quad (2)$$

Where,

θ = Angle of Repose

h = Powder particle pile height

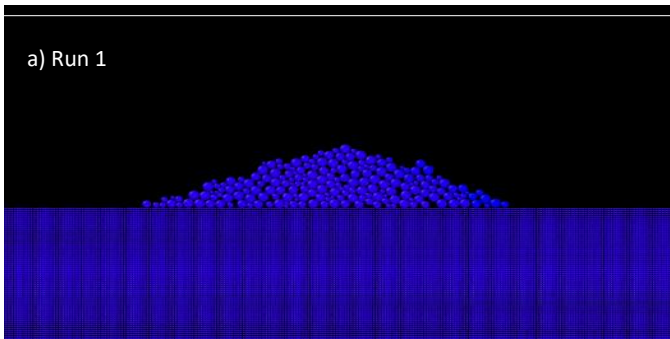
d = Diameter of the powder pile

The different particle ratios used for our work are listed in table 2. We limited our work to seven-sized particles for now. A diameter variation of 0.5 was used for the simulation. A ratio of diameters (2.5, 2.25, 2, 1.75, 1.5, 1.25, 1) is automatically detected in LAMMPS if we put these diameters in the input file.

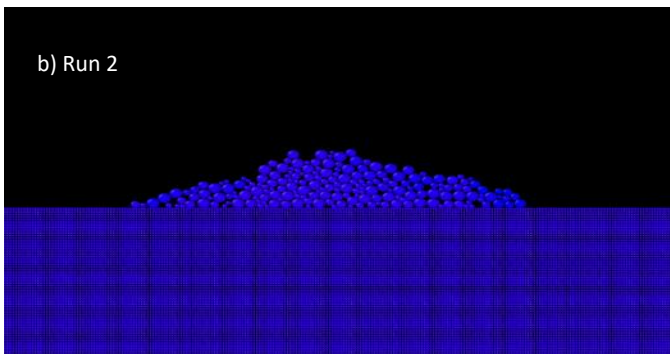
Table 2: Different particle ratios with varying diameter used in the Simulation

	Diameter	5	4.5	4	3.5	3	2.5	2
Run 1	Particle ratio	0.3	0.2	0.1	0.1	0.1	0.1	0.1
Run 2		0.2	0.1	0.1	0.1	0.1	0.1	0.2
Run 3		0.15	0.1	0.1	0.2	0.0	0.2	0.15
Run 4		0.15	0.1	0.1	0.1	0.1	0.0	0.2

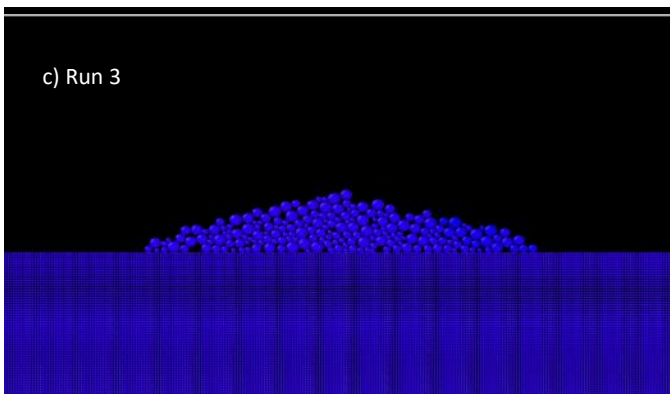
The angle of repose calculated for four different runs (Particle ratio variation) is illustrated in fig. 2.



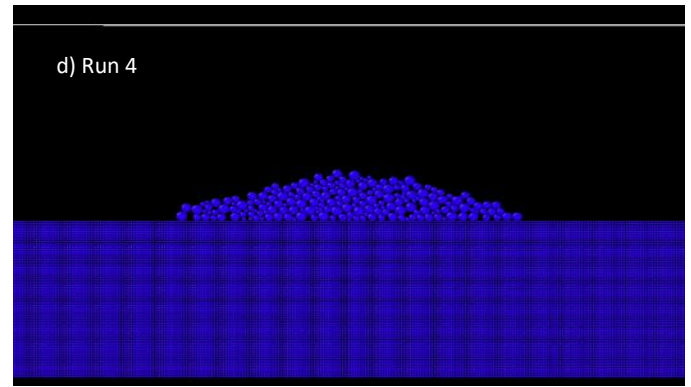
$$\theta = 22.469 \pm 0.5$$



$$\theta = 21.973 \pm 0.5^\circ$$



$$\theta = 19.7 \pm 0.5^\circ$$



$$\theta = 16.278 \pm 0.5^\circ$$

FIGURE 2: (a-d) Four different runs and their corresponding Angle of Repose

A combined graph that contains all the runs and their corresponding Angle of Repose (AOR) is shown in fig 3.

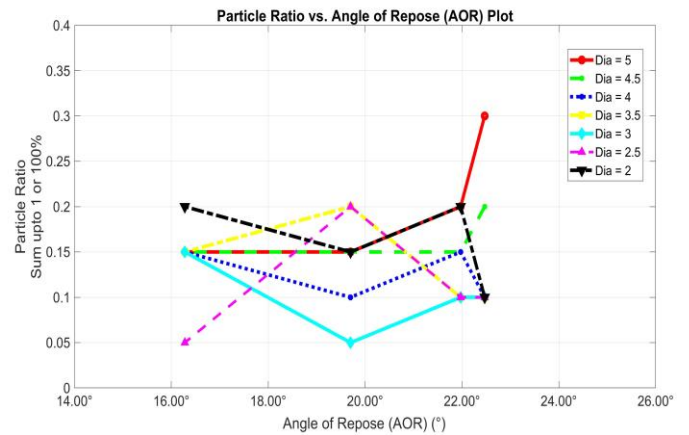


FIGURE 3: Particle ratio vs. Angle of Repose (AOR) Plot

From fig. 3, we can see that AOR is 16.278, which is the minimum AOR in the graph. The minimum AOR corresponds to a minimum particle ratio for larger-sized particles. Lower AOR means good flowability during the operation. When we set the particle ratio for larger-sized particles high, the AOR increases, which means that the flowability becomes poor which is in coherence with other research outcomes [28].

3.2 Influence of recoater shape

A recoater is mainly responsible for spreading powder particles over the substrate so that the printing process can take place. A couple of work has been done with the varying recoater shape and their influence on the bed [29][30]. In the powder bed system, recoater type and their spreading speed is an important factor as good spreading time can reduce the printing time. But if the spreading speed is high, it results in powder layer sparsing [31][17]. For our simulation, we considered a blade type and a

circular recoater. The recoating process for blade and circular type recoater at different timesteps is shown in fig. 4.

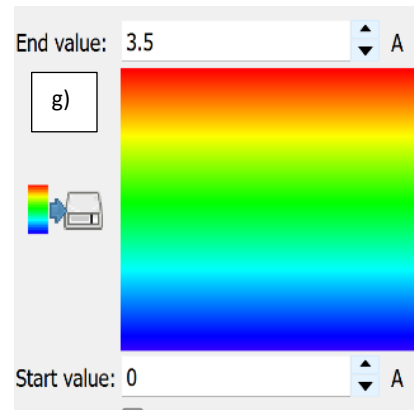
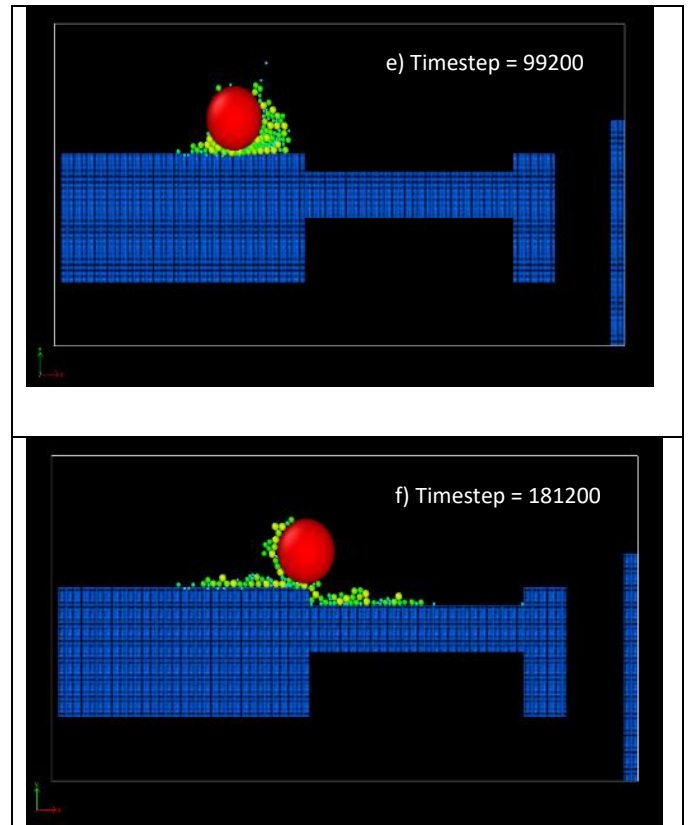
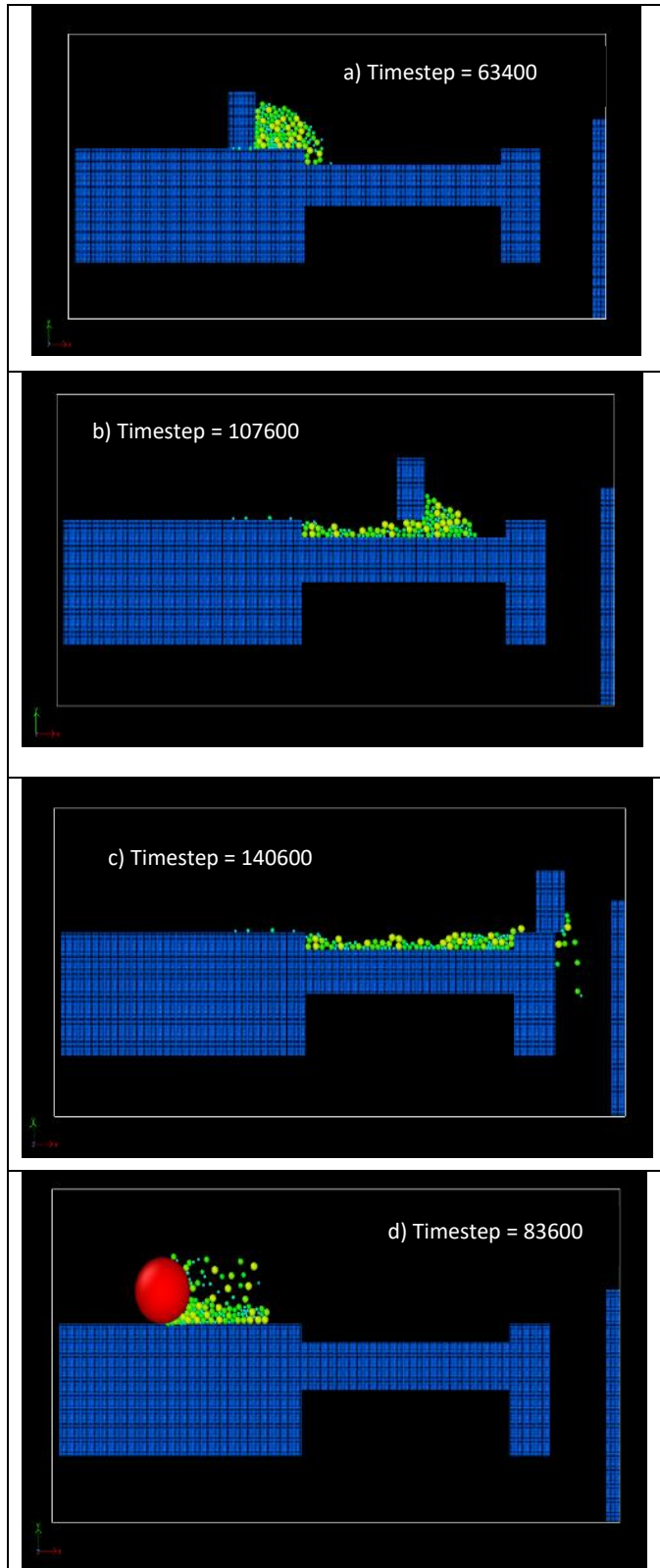


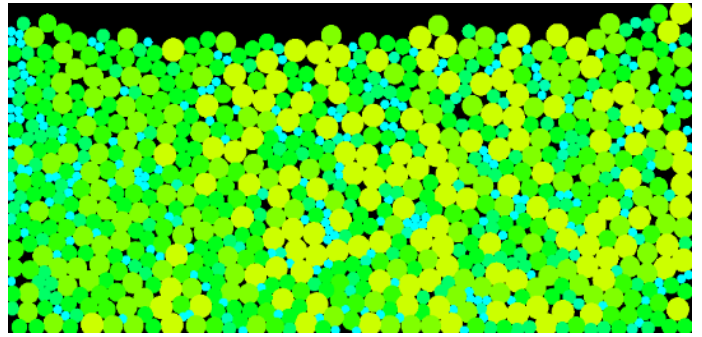
FIGURE 4: (a-c) Recoating action for blade type recoater (d-f) Recoating action for circular recoater (g) Colour coding values represent the radius

From fig. 4 (a-c), we can see that for blade type recoater the recoating process works smoothly, as a result, the powder bed was fully loaded with powders. On the other, there was an issue with the circular recoater (fig. 4 (d-f)), as we can see that the particles are attaching to the circular recoater which hinders the recoating process. But reducing the particle-particle interaction between recoater and powder particles would solve this kind of issue. The motion (rolling) of the circular recoater was set to 60 units so that it would not shoot those small particles. Whereas the motion of the blade recoater was 2.9 units. For color gradient (fig. (g)), a normalized value converted from the start

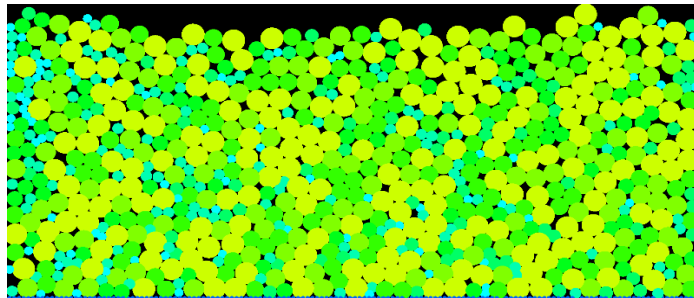
and end value is mapped into an RGB value depending on the selected color gradient. We used rainbow color gradient for our simulation.

3.3 Packing fraction

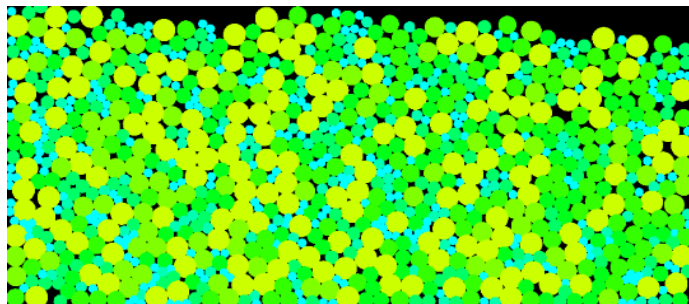
Packing fraction plays a pivotal role as it directly affects the mechanical and physical properties of any product [32]. A high packing fraction means the powder bed compaction is good. We know that the maximum packing fraction can be increased by introducing more smaller particles in the simulation box. Experimentally researchers showed that the size ratios above a critical value of smaller particles will not affect the packings of larger particles [33]. For four different runs (blade recoater used), we investigated the packing fraction of the powder bed which is illustrated in fig. 5.



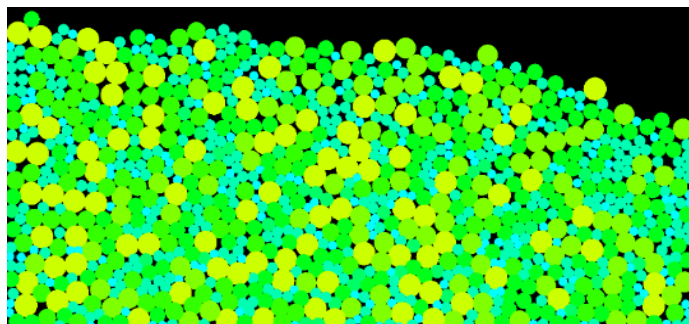
(d) Run 4



(a) Run 1



(b) Run 2



(c) Run 3

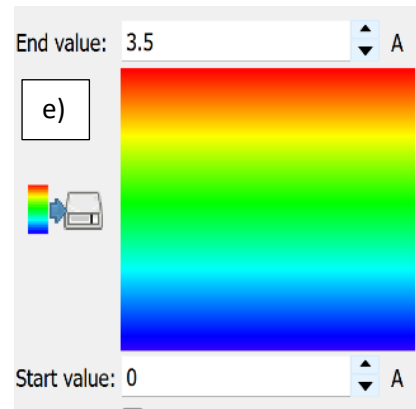


FIGURE 5: (a-d) Packing conditions for four different runs (e) Colour coding values represent the radius

We developed a code using Python using the OpenCV package and analyzed the packing fraction. For each run, we get a percentage of colors that are available in the powder bed. The higher percentage of black space means there is more empty space in the bed.

Table 3: Percentage of particles in Run 1

		Percentage (%)
Diameters	Empty space	13.449
	1	2.516
	1.5	4.248
	2.5	35.782
	2.25	18.814
	1.75	5.612
	1.25	5.383
	2	14.195

More number of bigger particles were detected by image processing for run 1. The empty space calculated for this run is 13.449 percent.

Table 4: Percentage of particles in Run 2

		Percentage (%)
Diameters	Empty space	12.012
	1	7.531
	1.5	8.051
	2.5	30.723
	2.25	12.432
	1.75	11.74
	1.25	4.096
	2	13.413

The empty space for run 2 was 12.012 percent. There were more smaller particles in run 2 which results in a decreased empty space.

Table 5: Percentage of particles in Run 3

		Percentage (%)
Diameters	Empty space	20.83
	1	4.220
	1.5	2.668
	2.5	17.251
	2.25	14.103
	1.75	15.846
	1.25	14.19
	2	10.89

The empty space for run 3 was 20.83 percent. There were more smaller particles in run 3 but the shaking of the bed agglomerates particles so that there was more empty space than in other runs.

Table 6: Percentage of particles in Run 4

		Percentage (%)
Diameters	Empty space	14.656
	1	5.003
	1.5	7.532
	2.5	23.684
	2.25	19.993
	1.75	14.964
	1.25	1.603
	2	12.563

The empty space for run 4 is 14.656 percent which is considerably less than run 3.

4. CONCLUSION

The powder spreading process in powder bed fusion has gained much interest among researchers in recent years which

in turn pushes many researchers to research the basic criteria of powder spreadability. As an instance, we tried to develop relationships among some parameters which characterize powder flowability, spreadability, packing fraction for Poly-disperse (Non-uniform) particles. Some critical observations from our research work are summarized as follows:

- 1) A higher amount of larger dia particles increase the AOR and thus affecting the flowability. So it's recommended to work with a proper mixer of different-sized powder particles that have a good flowability.
- 2) For circular recoater, the attraction and repulsion with the powder particles are very crucial during the spreading. It should be taken care of properly, otherwise, it would hinder the spreading process.
- 3) A combination of larger and smaller powder particles is helpful to get a better packing fraction. Increasing smaller particles largely may affect the powder bed when the bed goes down for another recoating cycle.

There should be more work with different sized particle ratios so that a critical value of the bigger particles can be suggested. Further work with a variety of ratios and their corresponding packing factor should be compared to each other to get the optimum packing factor. Besides, the load on the powder particles due to the recoater shape can be further analyzed for future work. Experimental work can also help bolster the simulation results, and that is what we are planning to do in the future.

ACKNOWLEDGEMENTS

This work is supported by the US Department of Defense Manufacturing Engineering Education Program (MEEP) under the award # N00014-19-1-2728.

REFERENCES

- [1] N. T. Aboulkhair, N. M. Everitt, I. Ashcroft, and C. Tuck, "Reducing porosity in AlSi10Mg parts processed by selective laser melting," *Addit. Manuf.*, vol. 1, pp. 77–86, 2014, doi: 10.1016/j.addma.2014.08.001.
- [2] F. J. Gürtler, M. Karg, M. Dobler, S. Kohl, I. Tzivilsky, and M. Schmidt, "Influence of powder distribution on process stability in laser beam melting: Analysis of melt pool dynamics by numerical simulations," *25th Annu. Int. Solid Free. Fabr. Symp. � An Addit. Manuf. Conf. SFF 2014*, no. July 2017, pp. 1099–1117, 2014.
- [3] W. Lee, YS; Zhang, "Mesoscopic simulation of heat transfer and fluid flow in laser Powder bed additive manufacturing," pp. 1154–1165.
- [4] S. Ziegelmeier *et al.*, "An experimental study into the effects of bulk and flow behaviour of laser sintering polymer powders on resulting part properties," *J.*

- Mater. Process. Technol.*, vol. 215, no. 1, pp. 239–250, Jan. 2015, doi: 10.1016/J.JMATPROTEC.2014.07.029.
- [5] W. Yan *et al.*, “An integrated process–structure–property modeling framework for additive manufacturing,” *Comput. Methods Appl. Mech. Eng.*, vol. 339, pp. 184–204, Sep. 2018, doi: 10.1016/J.CMA.2018.05.004.
- [6] W. Yan *et al.*, “Multi-physics modeling of single/multiple-track defect mechanisms in electron beam selective melting,” *Acta Mater.*, vol. 134, pp. 324–333, Aug. 2017, doi: 10.1016/J.ACTAMAT.2017.05.061.
- [7] W. E. King *et al.*, “Laser powder-bed fusion additive manufacturing of metals; physics, computational, and materials challenges,” *Addit. Manuf. Handb.*, pp. 461–502, Nov. 2018, doi: 10.1201/9781315119106-26.
- [8] M. Xia, D. Gu, G. Yu, D. Dai, H. Chen, and Q. Shi, “Porosity evolution and its thermodynamic mechanism of randomly packed powder-bed during selective laser melting of Inconel 718 alloy,” *Int. J. Mach. Tools Manuf.*, vol. 116, pp. 96–106, May 2017, doi: 10.1016/j.ijmachtools.2017.01.005.
- [9] M. Grasso and B. M. Colosimo, “Process defects and in situ monitoring methods in metal powder bed fusion: a review,” *Meas. Sci. Technol.*, vol. 28, no. 4, p. 044005, Feb. 2017, doi: 10.1088/1361-6501/AA5C4F.
- [10] A. L. Cooke and J. A. Slotwinski, “Properties of Metal Powders for Additive Manufacturing: A Review of the State of the Art of Metal Powder Property Testing,” Aug. 2012, doi: 10.6028/NIST.IR.7873.
- [11] B. Liu, R. Wildman, C. Tuck, I. Ashcroft, and R. Hague, “Investigation the effect of particle size distribution on processing parameters optimisation in selective laser melting process,” *22nd Annu. Int. Solid Free. Fabr. Symp. - An Addit. Manuf. Conf. SFF 2011*, pp. 227–238, 2011.
- [12] A. B. Spierings and G. Levy, “Comparison of density of stainless steel 316L parts produced with Selective Laser Melting using different powder grades,” *20th Annu. Int. Solid Free. Fabr. Symp. SFF 2009*, pp. 342–353, 2009.
- [13] J. Zheng, W. B. Carlson, and J. S. Reed, “The packing density of binary powder mixtures,” *J. Eur. Ceram. Soc.*, vol. 15, no. 5, pp. 479–483, Jan. 1995, doi: 10.1016/0955-2219(95)00001-B.
- [14] N. P. Karapatis, G. Egger, P. E. Gyax, and R. Glardon, “Optimization of Powder Layer Density in Selective Laser Sintering,” 1999, doi: 10.26153/TSW/746.
- [15] R. Y. Yang, R. P. Zou, and A. B. Yu, “Computer simulation of the packing of fine particles,” *Phys. Rev. E*, vol. 62, no. 3, p. 3900, Sep. 2000, doi: 10.1103/PhysRevE.62.3900.
- [16] J. Whiting and J. Fox, “Characterization of feedstock in the powder bed fusion process: Sources of variation in particle size distribution and the factors that influence them,” *Solid Free. Fabr. 2016 Proc. 27th Annu. Int. Solid Free. Fabr. Symp. - An Addit. Manuf. Conf. SFF 2016*, pp. 1057–1068, 2016.
- [17] E. J. R. Parteli and T. Pöschel, “Particle-based simulation of powder application in additive manufacturing,” *Powder Technol.*, vol. 288, pp. 96–102, Jan. 2016, doi: 10.1016/J.POWTEC.2015.10.035.
- [18] H. Chen, Q. Wei, S. Wen, Z. Li, and Y. Shi, “Flow behavior of powder particles in layering process of selective laser melting: Numerical modeling and experimental verification based on discrete element method,” *Int. J. Mach. Tools Manuf.*, vol. 123, pp. 146–159, Dec. 2017, doi: 10.1016/j.ijmachtools.2017.08.004.
- [19] J. C. Tully, “Molecular dynamics with electronic transitions,” *J. Chem. Phys.*, vol. 93, no. 2, p. 1061, Aug. 1998, doi: 10.1063/1.459170.
- [20] S. Luding, “From Molecular Dynamics and Particle Simulations towards Constitutive Relations for Continuum Theory,” *Lect. Notes Comput. Sci. Eng.*, vol. 71, pp. 453–492, 2009, doi: 10.1007/978-3-642-03344-5_16.
- [21] A. P. Thompson *et al.*, “LAMMPS - a flexible simulation tool for particle-based materials modeling at the atomic, meso, and continuum scales,” *Comput. Phys. Commun.*, vol. 271, p. 108171, Feb. 2022, doi: 10.1016/J.CPC.2021.108171.
- [22] A. Stukowski, “Visualization and analysis of atomistic simulation data with OVITO—the Open Visualization Tool,” *Model. Simul. Mater. Sci. Eng.*, vol. 18, no. 1, p. 015012, Dec. 2009, doi: 10.1088/0965-0393/18/1/015012.
- [23] L. E. Silbert, D. Ertaş, G. S. Grest, T. C. Halsey, D. Levine, and S. J. Plimpton, “Granular flow down an inclined plane: Bagnold scaling and rheology,” *Phys. Rev. E*, vol. 64, no. 5, p. 051302, Oct. 2001, doi: 10.1103/PhysRevE.64.051302.
- [24] N. V. Brilliantov, F. Spahn, J. M. Hertzsch, and T. Pöschel, “Model for collisions in granular gases,” *Phys. Rev. E*, vol. 53, no. 5, p. 5382, May 1996, doi: 10.1103/PhysRevE.53.5382.
- [25] H. P. Zhang and H. A. Makse, “Jamming transition in emulsions and granular materials,” *Phys. Rev. E - Stat. Nonlinear, Soft Matter Phys.*, vol. 72, no. 1, p. 011301, Jul. 2005, doi: 10.1103/PHYSREVE.72.011301/FIGURES/13/MEDIUM.
- [26] A. B. Spierings, M. Voegtlin, T. Bauer, and K. Wegener, “Powder flowability characterisation methodology for powder-bed-based metal additive manufacturing,” *Prog. Addit. Manuf.*, vol. 1, no. 1–2, pp. 9–20, Jun. 2016, doi: 10.1007/S40964-015-0001-4/FIGURES/12.
- [27] “ISO - ISO 4490:2014 - Metallic powders — Determination of flow rate by means of a calibrated funnel (Hall flowmeter).” <https://www.iso.org/standard/65132.html> (accessed Nov. 28, 2021).

- [28] P. Tan, F. Shen, W. S. Tey, and K. Zhou, "A numerical study on the packing quality of fibre/polymer composite powder for powder bed fusion additive manufacturing," *Virtual Phys. Prototyp.*, vol. 16, no. S1, pp. S1–S18, 2021, doi: 10.1080/17452759.2021.1922965.
- [29] S. Haeri, "Optimisation of blade type spreaders for powder bed preparation in Additive Manufacturing using DEM simulations," *Powder Technol.*, vol. 321, pp. 94–104, Nov. 2017, doi: 10.1016/j.powtec.2017.08.011.
- [30] L. Wang, A. Yu, E. Li, H. Shen, and Z. Zhou, "Effects of spreader geometry on powder spreading process in powder bed additive manufacturing," *Powder Technol.*, vol. 384, pp. 211–222, 2021, doi: 10.1016/j.powtec.2021.02.022.
- [31] S. Haeri, Y. Wang, O. Ghita, and J. Sun, "Discrete element simulation and experimental study of powder spreading process in additive manufacturing," *Powder Technol.*, vol. 306, pp. 45–54, Jan. 2017, doi: 10.1016/j.powtec.2016.11.002.
- [32] C. Meier, R. Weissbach, J. Weinberg, W. A. Wall, and A. J. Hart, "Critical influences of particle size and adhesion on the powder layer uniformity in metal additive manufacturing," *J. Mater. Process. Technol.*, vol. 266, pp. 484–501, Apr. 2019, doi: 10.1016/j.jmatprotec.2018.10.037.
- [33] H. J. H. Brouwers, "Packing fraction of geometric random packings of discretely sized particles," *Phys. Rev. E - Stat. Nonlinear, Soft Matter Phys.*, vol. 84, no. 4, p. 042301, Oct. 2011, doi: 10.1103/PHYSREVE.84.042301/FIGURES/2/MEDIUM.